

Expanding Heteroscorpionates. Facile Synthesis of New Hybrid Scorpionate/Cyclopentadienyl Ligands and Their Lithium and Group 4 Metal Compounds: A Combined Experimental and Density Functional Theory Study

Antonio Otero,^{*,†} Juan Fernández-Baeza,^{*,†} Antonio Antiñolo,[†] Juan Tejada,[†]
Agustín Lara-Sánchez,[†] Luis F. Sánchez-Barba,^{†,‡} Margarita Sánchez-Molina,[†]
Ana M. Rodríguez,[†] Carles Bo,^{§,⊥} and Manuel Urbano-Cuadrado[§]

Departamento de Química Inorgánica, Orgánica y Bioquímica, Universidad de Castilla-La Mancha, 13071-Ciudad Real, Spain, Departamento de Química Inorgánica y Analítica, Universidad Rey Juan Carlos, Mostoles-28933-Madrid, Spain, Institute of Chemical Research of Catalonia (ICIQ), Avenida Països Catalans 16, 43007-Tarragona, Spain, and Departament de Química Física i Inorgànica, Universitat Rovira i Virgili, Campus Sescelades, Macelli Domingo s/n, 43007 Tarragona, Spain

Received April 24, 2007

The preparation of new hybrid scorpionate/cyclopentadienyl ligands in the form of the lithium derivatives [Li(bpzcp)(THF)] (**1**) [bpzcp = 2,2-bis(3,5-dimethylpyrazol-1-yl)-1,1-diphenylethylcyclopentadienyl] and [Li(bpztcp)(THF)] (**2**) [bpztcp = 2,2-bis(3,5-dimethylpyrazol-1-yl)-1-*tert*-butylethylcyclopentadienyl] or as a mixture of the two scorpionate/cyclopentadiene regioisomers (bpzcpH) 1-[2,2-bis(3,5-dimethylpyrazol-1-yl)-1-phenylethyl]-1,3-cyclopentadiene (**3a**) and 2-[2,2-bis(3,5-dimethylpyrazol-1-yl)-1-phenylethyl]-1,3-cyclopentadiene (**3b**) has been carried out by reaction of bis(3,5-dimethylpyrazol-1-yl)methane (bdmpzm) with BuⁿLi and 6,6-diphenylfulvene, 6-*tert*-butylfulvene, or 6-phenylfulvene, respectively. However, when this insertion reaction was carried out with 6,6-dimethylfulvene, the compound [Li(^{isopr}cp)(bdmpzm)(THF)] (**4**) [^{isopr}cp = isopropenylcyclopentadienyl] was obtained. Compounds **1** and **2** reacted with [TiCl₄(THF)₂] or [MCl₄] (M = Zr, Hf) to give the complexes [MCl₃(bpzcp)] (M = Ti, **5**; Zr, **6**; Hf, **7**) and [MCl₃(bpztcp)] (M = Ti, **8**; Zr, **9**; Hf, **10**). Similar reactions do not take place with the mixture of the two isomers **3a** and **3b**. However, when a THF solution of **3a–3b** and [MCl₄] (M = Zr, Hf) was heated under reflux, the complexes [MCl₃(bpzcp)] (M = Zr, **11**; Hf, **12**) [bpzcp = 2,2-bis(3,5-dimethylpyrazol-1-yl)-1-phenylethylcyclopentadienyl] were obtained. In addition, alkyl complexes [ZrClMe₂(bpztcp)] (**13**) and [ZrMe₃(bpztcp)] (**14**) were also prepared. The structures of these complexes have been determined by spectroscopic and DFT methods, and in addition, the X-ray crystal structures of **1**, **2**, **3b**, and **6** were also established.

Introduction

Cyclopentadienyl systems with an additional donor function are attracting increased interest in the chemistry of early transition metals because of their potential applications as catalysts in polymerization processes.¹ Ligands possessing both a cyclopentadienyl ring and heteroatoms connected by an appropriate spacer are receiving considerable interest in synthesis and catalysis, as they lead to significant changes in both steric and electronic effects on the metal centers.² Furthermore, the most recent strategy in the design and modification of catalysts for olefin polymerization have involved the development of non-

cyclopentadienyl-based complexes of group 4 metals, with particular attention focused on nitrogen- and/or oxygen-containing ligands.³ In this context, scorpionate ligands such as poly-(pyrazolyl)borates are also attractive ancillary ligands for the synthesis of transition metal complexes.⁴ More recently—and related with the tris(pyrazolyl)borates—new, mixed pyrazolyl/cyclopentadienyl ligands have been described.⁵ In this important field of ligand design, we have previously reported the synthesis

* Corresponding author. E-mail: antonio.otero@uclm.es.

[†] Universidad de Castilla-La Mancha.

[‡] Universidad Rey Juan Carlos.

[§] ICIQ.

[⊥] Universitat Rovira i Virgili

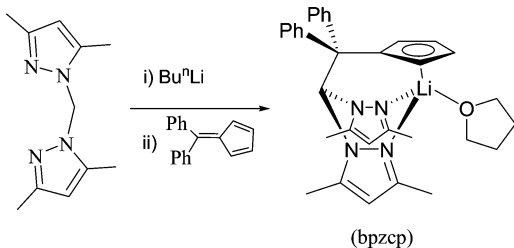
(1) See for example: (a) Deng, D.; Qian, C.; Wu, G.; Zheng, P. *J. Chem. Soc., Chem. Commun.* **1990**, 880–881. (b) Qian, C.; Wang, B.; Wu, G.; Zheng, P. *J. Organomet. Chem.* **1992**, 427, C29–C32. (c) Anwander, R.; Hermann, W. A.; Scherer, W.; Munck, F. C. *J. Organomet. Chem.* **1993**, 462, 163–174. (d) Molander, G.; Schumann, H.; Rosenthal, E. C. E.; Demtschuk, J. *Organometallics* **1996**, 15, 3817–3824. (e) Schumann, H.; Rosenthal, E. C. E.; Demtschuk, J. *Organometallics* **1998**, 17, 5324–5333. (f) Britovsek, G. J. P.; Gibson, V. C.; Wass, D. F. *Angew. Chem., Int. Ed.* **1999**, 38, 428–447. (g) Gibson, V. C.; Spitzmesser, S. K. *Chem. Rev.* **2003**, 103, 283–315.

(2) See for example: (a) McKnight, A. L.; Waymouth R. M. *Chem. Rev.* **1998**, 98, 2587–2598. (b) Siemeling, U. *Chem. Rev.* **2000**, 100, 1495–1526. (c) Butenschön, H. *Chem. Rev.* **2000**, 100, 1527–1564. (d) Qian, Y.; Huang, J.; Bala, M. D.; Lian, B.; Zhang, H.; Zhang, H. *Chem. Rev.* **2003**, 103, 2633–2690.

(3) See, for example: (a) Scollard, J. D.; McConville, D. H. *J. Am. Chem. Soc.* **1996**, 118, 10008–10009. (b) Scollard, J. D.; McConville, D. H.; Vittal, J. J. *Organometallics* **1997**, 16, 4415–4420. (c) Fokken, S.; Spaniol, T. P.; Okuda, J.; Serentz, F. G.; Mullhaupt, R. *Organometallics* **1997**, 16, 4240–4242. (d) Gibson, V. C.; Kimberly, B. S.; White, A. J. R.; Williams, D. J.; Houd, P. *Chem. Commun.* **1998**, 313–314. (e) Warren, T. H.; Schrock, R. R.; Davis W. M. *Organometallics* **1998**, 17, 308–321.

(4) (a) Trofimenko, S. *Scorpionates. The Coordination Chemistry of Polypyrazolylborate Ligands*; Imperial College Press: London, 1999. (b) Etienne, M.; Donnadieu, B.; Mathieu, R.; Fernández-Baeza, J.; Jalón, F. A.; Otero, A.; Rodrigo-Blanco, M. E. *Organometallics* **1996**, 15, 4597–4603. (c) Antiñolo, A.; Carrillo-Hermosilla, F.; Fernández-Baeza, J.; Lanfranchi, M.; Lara-Sánchez, A.; Otero, A.; Palomares, E.; Pellinghelli, M. A.; Rodríguez, A. M. *Organometallics* **1998**, 17, 3015–3019.

Scheme 1. Synthesis of the First Hybrid Scorpionate/Cyclopentadienyl Lithium Precursor of the Ligand Bpzcp

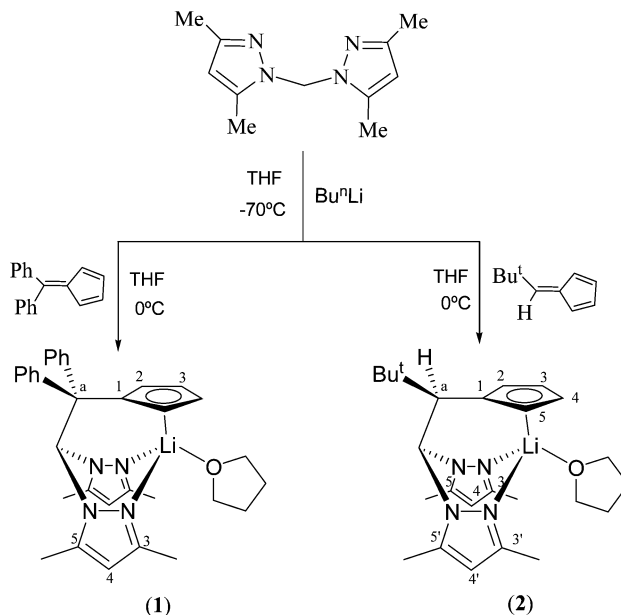


of new “heteroscorpionate” ligands based on bis(pyrazol-1-yl)methane,⁶ and these contain two pyrazole rings and a carboxylate, dithiocarboxylate, or methoxide group. These classes of tridentate ligands can coordinate to a wide variety of elements, e.g., from early to late transition metals. We have reported heteroscorpionate complexes containing group 4 and 5 metals,⁷ and more recently, we developed the synthesis of the first complexes of scandium and yttrium with these heteroscorpionate ligands.⁸

However, despite the development of donor-functionalized cyclopentadienyl ligands and the emerging importance of the “heteroscorpionate” ligands, hybrid scorpionate/cyclopentadienyl lithium precursors for the introduction of this type of ligand into transition metal complexes were unknown until we recently published the first hybrid scorpionate/cyclopentadienyl ligand.⁹ The unprecedented preparation of this new class of tridentate ligand [bpzcp = 2,2-bis(3,5-dimethylpyrazol-1-yl)-1,1-diphenylethylcyclopentadienyl] by a simple and efficient synthetic route led us to develop and fully explore the potential offered by this type of ligand (Scheme 1).

Herein we describe the synthesis and structural characterization of the lithium salts of several hybrid scorpionate/cyclopentadienyl ligands by a simple one-pot procedure, which opens up a new, broad way to prepare this type of interesting ligand. In addition, two of the compounds prepared contain a chiral center in the backbone of the ligand; thus the introduction of chirality into these systems opens the possibility of obtaining new enantiopure scorpionate ligands¹⁰ in the future, and these

Scheme 2. Synthesis of [Li(bpzcp)(THF)] (1) and [Li(bpztcp)(THF)] (2)



have potential uses in asymmetric catalysis. These ligands have been coordinated to group 4 metals, and a new series of hybrid scorpionate/cyclopentadienyl complexes for these elements were isolated and characterized. The reactivity of some of these toward alkylating lithium reagents has also been studied. Some structures were determined by means of a DFT-based method, which was also applied to discuss the nature of the metal–ligand interaction.

Results and Discussion

Ligand Syntheses. Deprotonation at the methylene group of bis(3,5-dimethylpyrazol-1-yl)methane (bdmpzm)¹¹ with BuⁿLi, followed by reaction with 6,6-diphenylfulvene or 6-*tert*-butylfulvene,¹² yielded the lithium compounds [Li(bpzcp)(THF)] (1) [bpzcp = 2,2-bis(3,5-dimethylpyrazol-1-yl)-1,1-diphenylethylcyclopentadienyl] and [Li(bpztcp)(THF)] (2) [bpztcp = 2,2-bis(3,5-dimethylpyrazol-1-yl)-1-*tert*-butylethylcyclopentadienyl] as colorless and orange solids, respectively, in good yield (ca. 85%) after the appropriate workup (see Scheme 2). However, when the same reaction was carried out with 6-phenylfulvene,¹² a mixture of two scorpionate/cyclopentadiene regioisomers (bpzpcpH), 1-[2,2-bis(3,5-dimethylpyrazol-1-yl)-1-phenylethyl]-1,3-cyclopentadiene (**3a**) and 2-[2,2-bis(3,5-dimethylpyrazol-1-yl)-1-phenylethyl]-1,3-cyclopentadiene (**3b**), was isolated as colorless solids (see Schemes 3). Although the latter reaction was carried out in anhydrous THF, a hydrolysis process from the adventitious water in the workup occurred. These compounds (**3a**, **3b**) are the first examples of bis(pyrazol-1-yl)methanes to contain a cyclopentadiene moiety in the carbon bridge. The deprotonation of **3** with BuⁿLi was also carried out, but the expected lithium scorpionate/cyclopentadienyl compound was not isolated, because an uncontrolled hydrolysis process in the workup occurred to give **3** again.

Finally, when the insertion process was carried out with 6,6-dimethylfulvene, a cyclopentadienyl lithium complex, [Li(^{isop}-

(5) (a) Lopes, I.; Lin, G. Y.; Domingos, A.; McDonald, R.; Marques, N.; Takats, J. *J. Am. Chem. Soc.* **1999**, *121*, 8110–8111. (b) Roitershtein, D.; Domingos, A.; Marques, N. *Organometallics* **2004**, *23*, 3483–3487.

(6) (a) Otero, A.; Fernández-Baeza, J.; Antiñolo, A.; Tejada J.; Lara-Sánchez, A. *Dalton Trans.* **2004**, 1499–1510 (perspective article). (b) Pettinari, C.; Pettinari, R. *Coord. Chem. Rev.* **2005**, *249*, 663–691.

(7) For group 5 metal complexes see for example: (a) Otero, A.; Fernández-Baeza, J.; Tejada, J.; Antiñolo, A.; Carrillo-Hermosilla, F.; Díez-Barra, E.; Lara-Sánchez, A.; Fernández-Lopez, M.; Lanfranchi M.; Pellinghelli, M. A. *J. Chem. Soc., Dalton Trans.* **1999**, 3537–3539. (b) Otero, A.; Fernández-Baeza, J.; Antiñolo, A.; Tejada, J.; Lara-Sánchez, A.; Sánchez-Barba, L.; Rodríguez, A. M. *Eur. J. Inorg. Chem.* **2004**, 260–266. For group 4 metal complexes see for example: (c) Otero, A.; Fernández-Baeza, J.; Antiñolo, A.; Carrillo-Hermosilla, F.; Tejada, J.; Díez-Barra, E.; Lara-Sánchez, A.; Sánchez-Barba, L.; López-Solera, I.; Ribeiro M. R.; Campos, J. M. *Organometallics* **2001**, *20*, 2428–2430. (d) Otero, A.; Fernández-Baeza, J.; Antiñolo, A.; Tejada, J.; Lara-Sánchez, A.; Sánchez-Barba, L.; Fernández-López M.; López-Solera, I. *Inorg. Chem.* **2004**, *43*, 1350–1358.

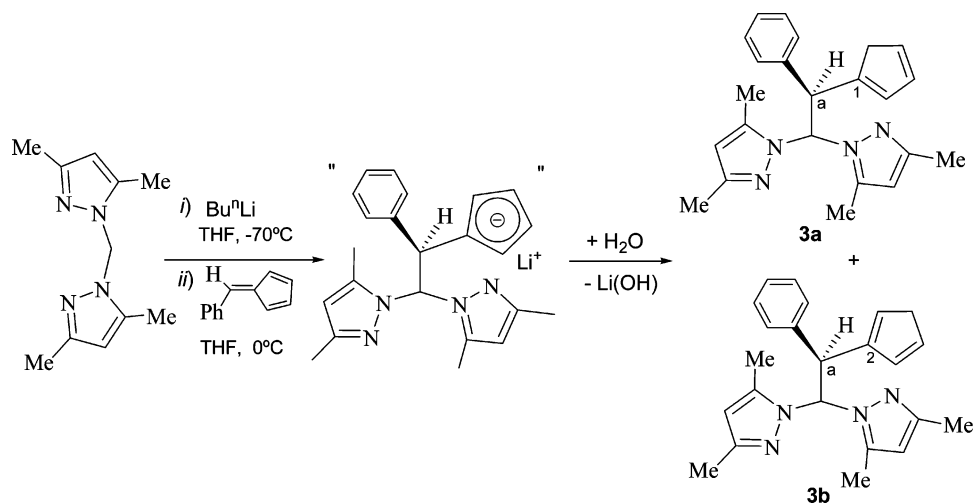
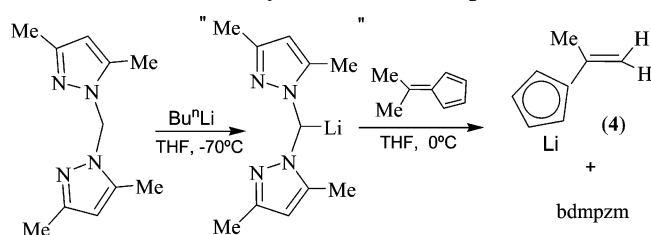
(8) Otero, A.; Fernández-Baeza, J.; Antiñolo, A.; Tejada, J.; Lara-Sánchez, A.; Sánchez-Barba, L.; Martínez-Caballero, E.; Rodríguez, A. M.; Lopez-Solera, I. *Inorg. Chem.* **2005**, *44*, 5336–5344.

(9) Otero, A.; Fernández-Baeza, J.; Antiñolo, A.; Tejada, J.; Lara-Sánchez, A.; Sánchez-Barba, L.; Rodríguez, A. M.; Maestro, M. A. *J. Am. Chem. Soc.* **2004**, *126*, 1330–1331.

(10) (a) Otero, A.; Fernández-Baeza, J.; Antiñolo, A.; Tejada, J.; Lara-Sánchez, A.; Sánchez-Barba, L.; Sanchez-Molina, M.; Franco, S.; Lopez-Solera, I.; Rodríguez A. M. *Eur. J. Inorg. Chem.* **2006**, 707–710 (Short Communication). (b) Otero, A.; Fernández-Baeza, J.; Antiñolo, A.; Tejada, J.; Lara-Sánchez, A.; Sánchez-Barba, L.; Sanchez-Molina, M.; Franco, S.; Lopez-Solera, I.; Rodríguez A. M. *Dalton Trans.* **2006**, 4359–4370.

(11) (a) Sebastian, J.; Sala, P.; Del Mazo, J.; Sancho, M.; Ochoa, C.; Elguero, J.; Fayet J. P.; Vertut, M. C. *J. Heterocycl. Chem.* **1982**, *19*, 1141–1145. (b) Díez-Barra, E.; de la Hoz, A.; Sánchez-Migallon A.; Tejada, J. *J. Chem. Soc., Perkin Trans. 1* **1993**, 1079–1083.

(12) Stone, K. J.; Little, R. D. *J. Org. Chem.* **1984**, *49*, 1849–1853.

Scheme 3. Synthesis of the Scorpionate/Cyclopentadiene Compounds **3a** and **3b** (bpzpcpH)Scheme 4. Synthesis of $[\text{Li}^{\text{isopr}}\text{cp}]$ (**4**)

cp]) (**4**) [isoprcp = isopropenylcyclopentadienyl], was obtained as a white solid (Scheme 4). The preparation of **4** involved the deprotonation of a methyl group of the fulvene by the bis-(pyrazol-1-yl)methylithium. This type of reaction has been described previously on using different organolithium reagents.¹³

At this point, it is worth mentioning the differences in the reactivities of the fulvenes in the processes described above. In fact, with 6,6-diphenylfulvene and 6-*tert*-butylfulvene the corresponding lithium scorpionate/cyclopentadienyl derivatives **1** and **2** were isolated, while with 6-phenylfulvene a similar lithium compound has been shown to be unstable to hydrolysis and a scorpionate/cyclopentadiene derivative **3** was the only isolable compound. It is possible that electronic effects due to the substituents on the fulvene carbon atom play an important role in the stabilization of the lithium scorpionate/cyclopentadienyl derivatives, meaning that the choice of substituents would be critical in designing a successful synthetic route. Indeed, the effects of the fulvene carbon atom substituents on the geometry of the scorpionate/cyclopentadiene ligand were investigated by determining the structures of isolated scorpionate/cyclopentadienyl ligands as well as their lithium derivatives. The geometric parameter that changes most is the bond angle of the fulvene carbon, since the values calculated for fulvene (122.9°), a 6-phenylfulvene (120.3°), and a 6,6-diphenylfulvene (113.9°) (as isolated ligands) show a clear trend. A similar trend was also found in the lithium derivatives (118.5°, 116.2°, 111.9°) (vide supra), and the low stability of the 6-phenylfulvene derivative may be related to pure electronic effects.

The different compounds were characterized spectroscopically. The mass spectra (FAB) of **1** and **2** indicate a mononuclear formulation. The ^1H and $^{13}\text{C}\{^1\text{H}\}$ NMR spectra of **1** show only

one set of resonances for the pyrazole rings, indicating that the pyrazoles are equivalent, and two multiplets for the cyclopentadienyl protons in ^1H NMR. These results are consistent with a tetrahedral disposition in which a symmetry plane exists that contains the lithium atom, the bridging carbons of the pyrazolyl rings, and atoms C^a and C^b (Scheme 2). However, the ^1H and $^{13}\text{C}\{^1\text{H}\}$ NMR spectra of **2** exhibit two distinct sets of pyrazole resonances, indicating the existence of two types of pyrazole rings. Furthermore, the ^1H NMR spectrum shows four multiplets for the cyclopentadienyl protons. A tetrahedral environment for the lithium atom can be proposed in which the two pyrazole rings are located in *cis* and *trans* positions with respect to the *tert*-butyl group (see Scheme 2). The phase-sensitive ^1H NOESY-1D spectra were also obtained in order to confirm the assignments of the signals for the Me^3 , Me^5 , and H^4 groups of each pyrazole ring. In this complex the carbon atom (C^a) is a stereogenic center, and we confirmed the presence in solution of the corresponding two enantiomers by adding a chiral shift reagent, namely, (*R*)-(-)-(9-anthryl)-2,2,2-trifluoroethanol. This process gave rise to two signals for each proton in the ^1H NMR spectrum, resulting from the two diastereoisomers of the corresponding two enantiomers. In addition, X-ray diffraction studies on **1** and **2** were carried out (see Figures 1 and 2). X-ray crystal studies on organolithium compounds containing carbon rings with delocalized π -electrons, such as benzyl, fluorenyl, and cyclopentadienyl, have been carried out, and a variety of η^2 -, η^3 -, and η^5 -bonding arrangements have been described.¹⁴ In this field, additional structural studies on other related compounds, such as **1** and **2**, would be quite useful in helping to further define the bonding in these complexes. The most representative bond lengths and angles are presented in Table 1. Both complexes have a monomeric structure. In both complexes the geometry around the Li atom can be described as a distorted tetrahedron with a "heteroscorpionate" ligand that acts in a tridentate fashion (two coordinated pyrazole rings and a cyclopentadienyl ring) and one molecule of THF. The Li–N distances [2.37(1) and 2.13(1) Å] for **1** and [2.150(5) and 2.131(5) Å] for **2** are in good agreement with others determined for lithium scorpionate or poly(pyrazolyl)methane complexes.^{7a,15} The C_5H_4 ring is unsymmetrically bonded to the Li atom with Li–C bond lengths ranging from 2.25(1) to 2.50(6) Å. The X-ray diffraction study confirms that the presence in solution

(13) (a) Macomber, D. W.; Hart, W. P.; Rausch, M. D. *J. Am. Chem. Soc.* **1982**, *104*, 884–886. (b) Knüppel, S.; Erker, G.; Fröhlich, R. *Angew. Chem., Int. Ed.* **1999**, *38*, 1923–1926. (c) Bai, S. D.; Wei, X. H.; Guo, J. P.; Liu, D. S.; Zhou, Z. Y. *Angew. Chem., Int. Ed.* **1999**, *38*, 1926–1928.

(14) (a) Qian, B.; Henling, L. M.; Peters, J. C. *Organometallics* **2000**, *19*, 2805–2808. (b) Culp, R. D.; Cowley, A. H. *Organometallics* **1996**, *15*, 5380–5384.

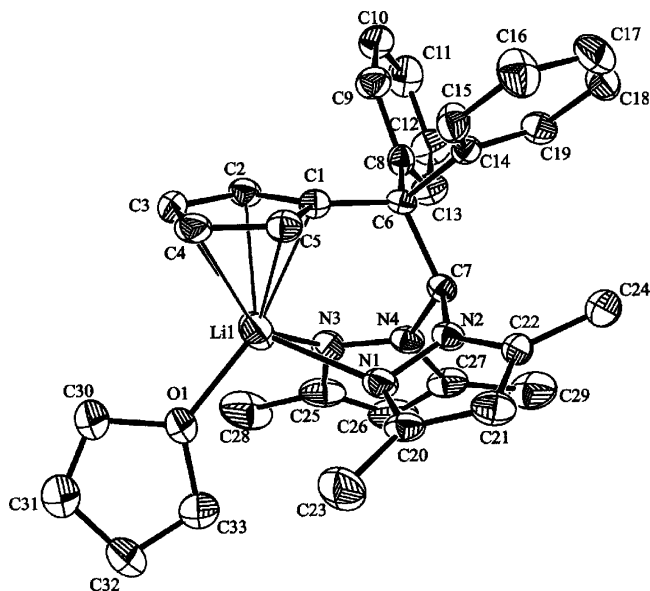


Figure 1. ORTEP view of [Li(bpzcp)(THF)] (**1**). Ellipsoids are at the 30% probability level, and hydrogen atoms have been omitted for clarity.

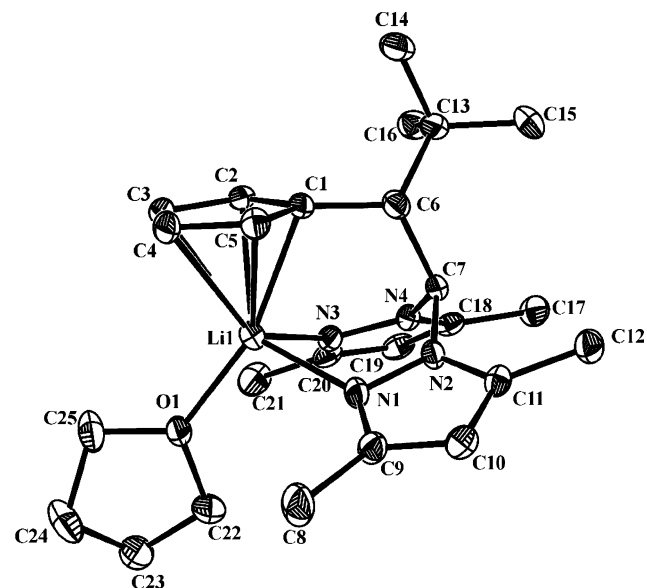


Figure 2. ORTEP view of [Li(S-bpztpc)(THF)] (**2**). Ellipsoids are at the 30% probability level, and hydrogen atoms have been omitted for clarity.

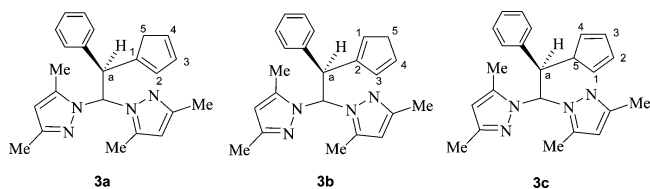


Figure 3. Proposed structures for the three isomers of compound **3**.

of the corresponding two enantiomers for complex **2** (*R* + *S*) is maintained in the solid state.

Selected geometrical parameters are given in Table 1 for the DFT-optimized structure of a model of **1** and **2** in which the

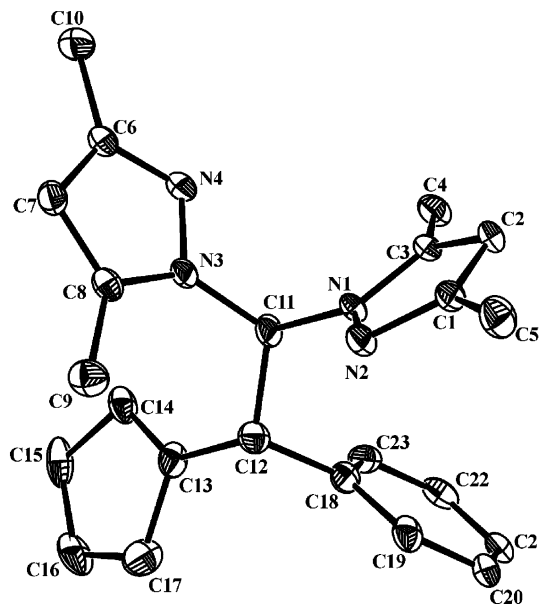


Figure 4. ORTEP view of 1,1'-[2-(1,3-cyclopentadien-2-yl)-2-phenylethylidene]bis(3,5-dimethylpyrazole) (**3b**). Ellipsoids are at the 30% probability level, and hydrogen atoms have been omitted for clarity.

substituents at C(6) were either two hydrogen atoms, one hydrogen atom and one phenyl group, or two phenyl groups. The agreement between the X-ray results and the computed values is remarkable. When $R_1 = R_2 = \text{H}$, the shortest Li–C(Cp) distance corresponds to the Li–C(1) bond (2.262 Å), while the bond lengths to C(2) (2.377 Å) and C(5) (2.376 Å) are slightly longer but equivalent. The same trend is observed for Li–C(3) and Li–C(4), and this indicates that the Cp ring lies horizontal and symmetric on top of the Li atom. The geometry of this model compound matches perfectly well the X-ray parameters obtained for compound **2**. It is worth noting that since the angle C(1)–C(6)–C(7) is calculated as being slightly wider than its value in **2**, all the computed carbon–lithium bonds are calculated as being slightly longer. As we mentioned above, the nature of substituents on the fulvene carbon affects, to a large extent, the bond angle of the isolated ligands as well as the angle C(1)–C(6)–C(7) in the Li complexes. Note that this angle became narrower when H atoms were substituted by phenyl groups. An additional effect was observed in the molecular structure of compounds **1** and **2**: the rotation of the Cp ring around the C(1)–C(6) bond that breaks the symmetry in the Li–C(Cp) bond distances. This is clearly visible in the difference between the Li–C(3) and Li–C(4) bond lengths in **1** and **2**, but also in the computed structures when $R_1 = \text{H}$ and $R_2 = \text{Ph}$ and when $R_1 = R_2 = \text{Ph}$. This tilting results in a shorter Li–C(5) bond distance that in **1** is indeed the shortest lithium–carbon bond. Also, the computed values reproduce fairly well these features. Although the computed values are not able to reproduce the Li–C(5) bond as the shortest, the difference between the Li–C(1) and the Li–C(5) is rather small. Indeed, the Li–C(1) is the only carbon–lithium bond that is characterized by the presence of a bond critical point in the electronic charge density function.¹⁶

In the hydrolysis process that leads to compound **3** it is possible to form three isomers (see Figure 3). Two sets of ¹H NMR signals are observed for this mixture, which is consistent with the presence of only two tautomers. In both compounds

(15) (a) Otero, A.; Fernández-Baeza, J.; Tejada, J.; Antiñolo, A.; Carrillo-Hermosilla, F.; Díez-Barra, E.; Lara-Sánchez, A.; Fernández-Lopez, M. *J. Chem. Soc., Dalton Trans.* **2000**, 2367–2374. (b) Reger, D. L.; Collins, J. E.; Matthews, M. A.; Rheingold, A. L.; Liable-Sands, L. M.; Guzei, I. A. *Inorg. Chem.* **1997**, *36*, 6266–6269.

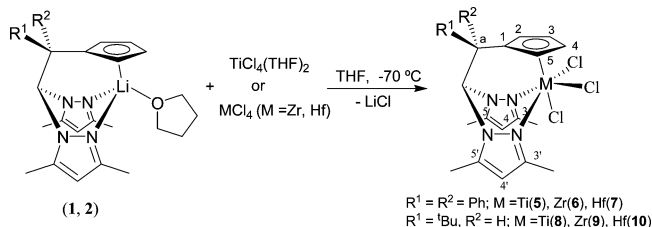
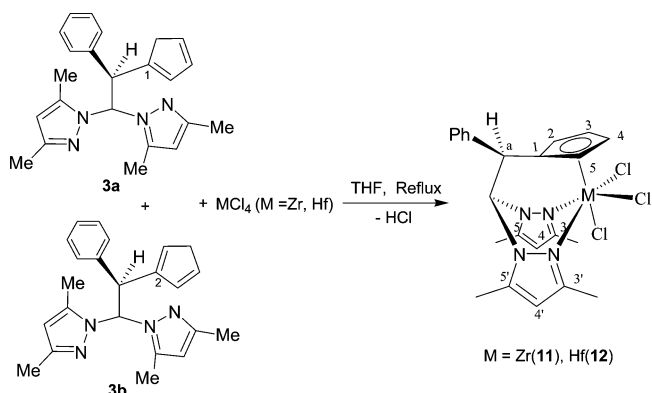
(16) Bader, R. W. F. *Atoms in Molecules: A Quantum Theory*; Clarendon Press, 1994.

Table 1. Selected Geometrical Parameters for the X-ray Studies of **1**, **2**, and **3b** and for Computed Structures of Models of **1** and **2** (distances in Å, angles in deg)

1 (R ₁ = R ₂ = Ph)			2 (R ₁ = H, R ₂ = ^t Bu)			2 (R ₁ = R ₂ = H)			2 (R ₁ = H, R ₂ = Ph)			3b		
exp			calc			exp			calc			exp		
Bond Lengths														
Li(1)–O(1)	1.96(1)	2.103	Li(1)–O(1)	1.968(5)	2.028	2.055	N(1)–C(11)					1.457(3)		
Li(1)–N(1)	2.37(1)	2.196	Li(1)–N(1)	2.150(5)	2.188	2.235	N(3)–C(11)					1.458(3)		
Li(1)–N(3)	2.13(1)	2.132	Li(1)–N(3)	2.131(5)	2.210	2.174	C(11)–C(12)					1.514(4)		
Li(1)–C(1)	2.28(1)	2.270	Li(1)–C(1)	2.252(5)	2.262	2.260	C(12)–C(13)					1.503(4)		
Li(1)–C(2)	2.38(1)	2.340	Li(1)–C(2)	2.372(5)	2.377	2.429	C(12)–C(18)					1.539(4)		
Li(1)–C(3)	2.44(1)	2.415	Li(1)–C(3)	2.504(6)	2.521	2.544	C(13)–C(14)					1.355(4)		
Li(1)–C(4)	2.35(1)	2.389	Li(1)–C(4)	2.469(5)	2.521	2.461	C(13)–C(17)					1.477(4)		
Li(1)–C(5)	2.25(1)	2.294	Li(1)–C(5)	2.321(5)	2.376	2.290	C(14)–C(15)					1.496(4)		
N(2)–C(7)	1.462(6)	1.466	N(2)–C(7)	1.458(3)	1.459	1.463	C(15)–C(16)					1.439(5)		
N(4)–C(7)	1.463(6)	1.468	N(4)–C(7)	1.453(3)	1.459	1.459	C(16)–C(17)					1.396(5)		
C(1)–C(6)	1.520(7)	1.529	C(1)–C(6)	1.509(4)	1.499	1.507								
C(6)–C(7)	1.581(7)	1.626	C(6)–C(7)	1.570(4)	1.573	1.593								
Angles														
O(1)–Li(1)–N(3)	105.4(5)	104.3	O(1)–Li(1)–N(3)	103.6(2)	101.5	103.5	N(1)–C(11)–N(3)					110.5(2)		
O(1)–Li(1)–N(1)	103.5(5)	104.5	O(1)–Li(1)–N(1)	102.0(2)	102.2	102.8	N(1)–C(11)–C(12)					111.7(2)		
N(3)–Li(1)–N(1)	83.4(4)	86.5	N(3)–Li(1)–N(1)	85.9(2)	85.0	84.9	N(3)–C(11)–C(12)					116.4(2)		
C(1)–C(6)–C(7)	113.0(4)	111.9	C(1)–C(6)–C(7)	115.8(2)	118.5	116.2	C(13)–C(12)–C(11)					113.4(2)		
							C(13)–C(12)–C(18)					110.0(2)		
							C(11)–C(12)–C(18)					107.1(2)		

the H⁵ signal in the ¹H NMR spectrum integrates for two protons, meaning that the regioisomer **3c** [in which the cyclopentadiene group is bonded by C⁵ to the bis(pyrazol-1-yl)methane unit] can be ruled out. In the solid state one isomer was crystallized and characterized by X-ray diffraction (Figure 4). Selected bond lengths and angles are collected in Table 1. The short C(13)–C(14) [1.355(4) Å] and C(16)–C(17) [1.396(5) Å] distances are indicative of a double bond, whereas the C(14)–C(15) [1.496(4) Å], C(15)–C(16) [1.439(5) Å], and C(13)–C(17) [1.477(4) Å] distances are indicative of a single bond. These results are consistent with the structural disposition described for isomer **3b**. The C–C distances found in this cyclopentadiene moiety can be compared to those typically found for the classic cyclopentadiene.¹⁷ The pyrazole rings of this compound are orientated in a quasi-antiparallel manner with respect to each other, presumably to minimize the intramolecular steric interaction between the N(2) and N(4) atoms of the two rings. This conformation is similar to that found with the (2-hydroxyphenyl)bis(pyrazolyl)methane derivative.¹⁸ The cyclopentadiene and phenyl rings are probably in this quasi-antiparallel disposition to minimize steric interactions between the two rings.

Group 4 Halide Compounds. Having prepared this new class of hybrid scorpionate/cyclopentadienyl compounds in the form of their lithium salts, we explored their potential utility as tridentate ligands in the preparation of new group 4 metal complexes. Compounds **1–3** proved to be useful reagents for the synthesis of new titanium, zirconium, and hafnium complexes. The lithium compounds **1** and **2** were reacted at –70 °C with [TiCl₄(THF)₂] or [MCl₄] (M = Zr, Hf) in a 1:1 molar ratio in THF to give, after the appropriate workup, the complexes [MCl₃(bpzcp)] (M = Ti, **5**; Zr, **6**; Hf, **7**) and [MCl₃(bpztcp)] (M = Ti, **8**; Zr, **9**; Hf, **10**), which were isolated as red or orange solids in good yield (Scheme 5). An interesting reactivity was observed when a mixture of [MCl₄] (M = Zr, Hf) and **3a–3b** was heated under reflux for 12 h, as the new complexes [MCl₃-(bpzpcp)] (M = Zr, **11**; Hf, **12**) [bpzpcp = 2,2-bis(3,5-dimethylpyrazol-1-yl)-1-phenylethylcyclopentadienyl] were ob-

Scheme 5. Synthesis of Complexes [MCl₃(bpzcp)] (**5–7**) and [MCl₃(bpztcp)] (**8–10**)**Scheme 6.** Synthesis of Complexes [MCl₃(bpzpcp)] (**11** and **12**)

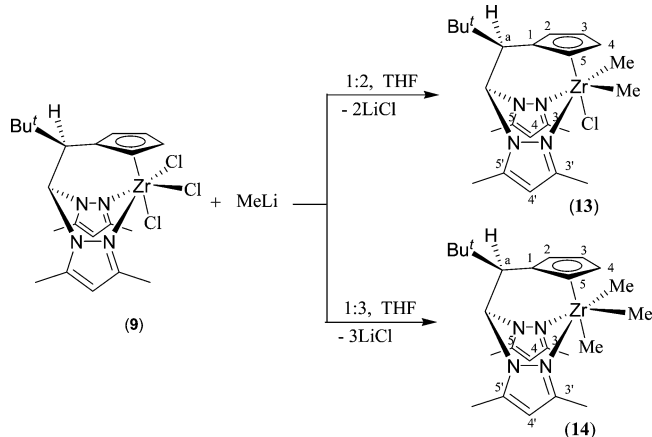
tained, after the appropriate workup procedure, as yellow and orange solids, respectively (Scheme 6). The analogous reaction with TiCl₄(THF)₂ gave a complex mixture of products that could not be separated. The preparation of **11** and **12** involved an unusual deprotonation of the cyclopentadiene moiety with the formation of hydrogen chloride. The deprotonation of cyclopentadiene is a well-known procedure, and it normally proceeds by either acid–base or protonolysis processes; for example, the reaction of scandium or yttrium tris(alkyl) complexes and cyclopentadiene gives the corresponding mono(cyclopentadienyl)metal-bis(alkyl) complexes with the elimination of an alkane.¹⁹ Furthermore, there are well-documented processes²⁰

(17) (a) Haumann, T.; Benet-Buchholz, J.; Boese, R. *J. Mol. Struct.* **1996**, *374*, 299–304. (b) Liebling, G.; Marsh, R. E. *Acta Crystallogr.* **1965**, *19*, 202–208.

(18) Higgs, T. C.; Carrano, C. J. *Inorg. Chem.* **1997**, *36*, 291–297.

(19) (a) Hultsch, K. C.; Spaniol, T. P.; Okuda, J. *Angew. Chem., Int. Ed.* **1999**, *38*, 227–230. (b) Li, X.; Baldamus, J.; Hou, Z. *Angew. Chem., Int. Ed.* **2005**, *44*, 962–965.

Scheme 7. Synthesis of Alkyl Complexes 13 and 14



in which the transformation of a cyclopentadiene to a cyclopentadienyl moiety is facilitated by the presence of a good leaving group, such as SiMe_3 in the form of SiMe_3Cl . However, the reaction reported here does not correspond to either of the processes outlined above. A novel and direct one-pot procedure has recently been published for the synthesis of monocyclopentadienyl titanium trichloride complexes with a side chain containing a group able to coordinate to the Ti center by reaction of TiCl_4 and several cyclopentadienes.²¹ Our process represents the second example of this interesting type of reactivity. As indicated above,²¹ the two pyrazole rings of **3a** and **3b** probably interact with the metal center (Zr or Hf) in a first step to give an intermediate in which the subsequent intramolecular reaction between the MCl_4^- and $-\text{C}_5\text{H}_5$ moieties may be favored and lead to the formation of the heteroscorpionate ligand with $\kappa^2\text{-NN}\eta^5\text{-Cp}$ coordination to the metal center.

The different group 4 metal complexes were characterized spectroscopically. The ^1H and $^{13}\text{C}\{\text{H}\}$ NMR spectra of **5–7** (nonchiral compounds) exhibit a singlet for each of the H^a , Me^3 , and Me^5 pyrazole protons, indicating that the pyrazoles are equivalent, along with two multiplets for the cyclopentadienyl protons. These results are consistent with an octahedral disposition in which a symmetry plane exists (see Scheme 5). The ^1H NMR spectra of complexes **8–12** (chiral compounds) show two singlets for each of the H^a , Me^3 , and Me^5 pyrazole protons and four multiplets for the H^c , H^d , H^e , and H^f cyclopentadienyl protons. These results also are consistent with an octahedral structural disposition where a $\kappa^2\text{-NN}\eta^5\text{-Cp}$ coordination for the scorpionate ligand is also proposed. The assignment of the $^{13}\text{C}\{\text{H}\}$ NMR signals was made on the basis of $^1\text{H}\text{-}^{13}\text{C}$ heteronuclear correlation (g-HSQC) experiments. In these asymmetric complexes we confirmed the presence in solution of the corresponding two enantiomers by addition of the chiral shift reagent discussed previously. Complexes **5–12** constitute the first examples of group 4 metal complexes bearing a hybrid scorpionate/cyclopentadienyl ligand.

In order to confirm the proposed structure for these complexes, an X-ray crystal structure analysis was carried out on complex **6** (see Figure 5). Selected bond lengths and angles are collected in Table 2. The structure consists of a heteroscorpionate ligand bonded to the zirconium atom through the two nitrogen atoms and the cyclopentadienyl ring in a $\kappa^2\text{-NN}\eta^5\text{-Cp}$ coordination mode. In addition, the zirconium center is coordi-

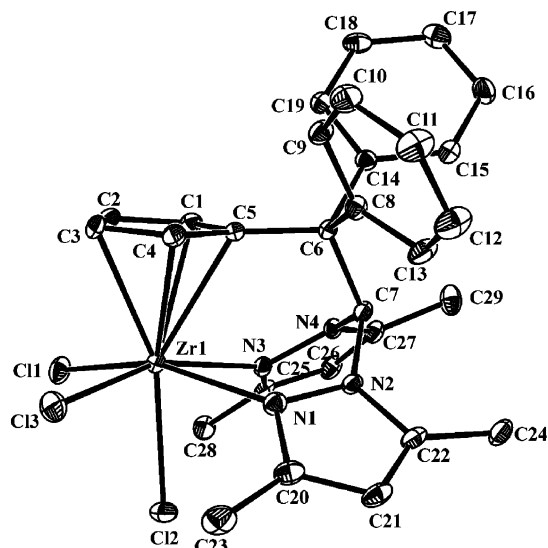


Figure 5. ORTEP view of $[\text{ZrCl}_3(\text{bpzcp})]$ (**6**). Ellipsoids are at the 30% probability level, and hydrogen atoms have been omitted for clarity.

inated to three chlorine atoms. This center has a distorted octahedral environment with a major distortion in the $\text{N}(1)\text{-Zr}(1)\text{-Cl}(1)$ angle, which has a value of $158.32(9)^\circ$. The $\text{Zr}(1)\text{-Cl}(1)$ and $\text{Zr}(1)\text{-Cl}(3)$ bond distances of 2.479(1) and 2.468(1) Å, respectively, are as one would expect for a Zr pyrazolyl complex,²² but the elongated $\text{Zr}(1)\text{-Cl}(2)$ distance of 2.513(1) Å indicates that the cyclopentadienyl ring exerts a *trans* influence. In this complex, in contrast to lithium complexes **1** and **2**, the C_5H_4 ring is symmetrically bonded to the metal center with $\text{Zr}\text{-C}$ bond distances of 2.523(4) to 2.572(4) Å.

The structures of complexes **5**, **6**, and **7** were obtained by means of full geometry optimizations at a DFT level. Initially we considered models of the real complexes in which $\text{R}_1 = \text{R}_2 = \text{H}$ and then investigated a full model of complex **6** ($\text{R}_1 = \text{R}_2 = \text{Ph}$). The data for complex **6** are collected in Table 2, and these show that the agreement between computed and X-ray values is fairly good, although the metal–nitrogen bond distances are slightly overestimated. The most striking difference is found in the $\text{C}(5)\text{-C}(6)\text{-C}(7)$ bond angle, which is 109.2° in the X-ray structure but is computed to be 116.4° in the model of complex **6**. However, when the full structure of complex **6** was considered, i.e., replacing the hydrogen substituents in $\text{C}(6)$ by phenyl groups, the computed value was almost identical to the experimental one. The origin of this effect is purely electronic, as stated above, since steric hindrance is not expected to play any role. Significant differences in the structures are not observed on going from the Ti to the Zr and Hf complexes (see data in Table 2), although there is a clear trend in the metal–nitrogen and metal–chlorine bond lengths $\text{Ti} < \text{Zr} \approx \text{Hf}$. As it was found in the lithium complexes, when $\text{R}_1 = \text{R}_2 = \text{H}$, the shortest distance between the metal (Ti, Zr, or Hf) and the cyclopentadienyl ligand corresponds to that with the $\text{C}(5)$ carbon atom, in disagreement with the X-ray structure of **6** (see Table 2). As it was found for complexes **1** and **2**, this was the only metal–carbon bond characterized by the presence of a bond critical point in the charge density. However, when $\text{R}_1 = \text{R}_2 = \text{Ph}$, and with the narrowing of the $\text{C}(5)\text{-C}(6)\text{-C}(7)$ angle and the tilting of the Cp ring, the zirconium atom became more centered in relation to the Cp ring, and as a consequence, the

(20) (a) Blais, M. S.; Chien, J. C. W.; Rausch, M. D. *Organometallics* **1998**, *17*, 3775–3783. (b) Zeijden, A. A. H.; Mattheis, C.; Fröhlich, R. *Organometallics* **1997**, *16*, 2651–2658.

(21) Zhang, Y.; Mu, Y. *Organometallics* **2006**, *25*, 631–634.

(22) Oshiki, T.; Mashima, K.; Kawamura, S.; Tani, K.; Kitaura, K. *Bull. Chem. Soc. Jpn.* **2000**, *73*, 1735–1748.

Table 2. Selected Geometrical Parameters for the X-ray Structure of **6** and for Computed Structures of Models of **5**, **6**, and **7**

	6 M = Zr R ₁ = R ₂ = Ph		6 M = Zr R ₁ = R ₂ = H		5 M = Ti R ₁ = R ₂ = H		7 M = Hf R ₁ = R ₂ = H	
	exp	calc	calc	calc	calc	calc	calc	
	Bond Lengths							
M(1)–N(3)	2.391(4)	2.524	2.576	2.517	2.551			
M(1)–N(1)	2.424(4)	2.530	2.557	2.528	2.570			
M(1)–Cl(3)	2.468(1)	2.489	2.483	2.353	2.480			
M(1)–Cl(1)	2.479(1)	2.498	2.492	2.361	2.488			
M(1)–Cl(2)	2.513(1)	2.508	2.499	2.380	2.497			
M(1)–C(1)	2.529(4)	2.614	2.628	2.515	2.627			
M(1)–C(2)	2.572(4)	2.644	2.682	2.588	2.681			
M(1)–C(3)	2.548(4)	2.636	2.678	2.580	2.676			
M(1)–C(4)	2.523(4)	2.593	2.627	2.509	2.625			
M(1)–C(5)	2.534(4)	2.630	2.603	2.489	2.602			
N(2)–C(7)	1.440(5)	1.458	1.452	1.451	1.452			
N(4)–C(7)	1.465(5)	1.465	1.457	1.455	1.457			
C(5)–C(6)	1.525(6)	1.531	1.499	1.499	1.500			
C(6)–C(7)	1.568(6)	1.591	1.540	1.536	1.539			
C(6)–C(8)	1.550(6)	1.560						
C(6)–C(14)	1.568(6)	1.571						
Angles								
N(3)–M(1)–N(1)	76.0(1)	74.1	71.0	73.7	72.1			
N(1)–M(1)–Cl(3)	91.27(9)	90.5	90.1	89.8	90.1			
N(3)–M(1)–Cl(1)	92.33(9)	93.5	94.3	92.9	94.3			
Cl(3)–M(1)–Cl(1)	94.70(5)	97.9	99.3	98.0	99.3			
N(3)–M(1)–Cl(2)	79.75(9)	78.8	78.5	77.0	78.4			
N(1)–M(1)–Cl(2)	78.06(9)	78.9	78.0	76.9	77.9			
Cl(3)–M(1)–Cl(2)	83.42(5)	86.3	86.2	84.8	86.2			
Cl(1)–M(1)–Cl(2)	81.94(4)	84.5	84.6	83.9	84.6			
C(5)–C(6)–C(7)	109.2(3)	110.3	116.4	115.8	116.3			
N(2)–C(7)–N(4)	109.3(3)	110.9	112.4	112.6	112.2			
N(2)–C(7)–C(6)	114.6(3)	115.2	113.0	112.4	113.0			
N(4)–C(7)–C(6)	112.9(3)	113.7	113.2	112.7	113.2			

Zr–C(1) and Zr–C(4) bonds became the shortest, in accordance with X-ray values. Indeed, bond critical points corresponding to the three Zr–C(1), Zr–C(4), and Zr–C(5) bonds were characterized when the topological analysis of the electronic charge density function was carried out for the computed structure of **6**. Hence, although simple models were able to capture the essential features of these scorpionate/cyclopentadienyl compounds, subtle effects such as those arising from substitution on the fulvene carbon are required to take into account the whole structure of the complexes.

Several issues regarding the structure and the nature of the bonding between the scorpionate/cyclopentadienyl ligands and the lithium and group 4 metal centers are discussed below. The geometric parameters shown in Tables 1 and 2 for our model systems indicate that, as one would expect, the metal–carbon bond distances are slightly shorter in the lithium complex than the titanium system, although this difference is not large. The difference is related to the bending angle of the ligand C(1)–C(6)–C(7) or C(5)–C(6)–C(7) and to the pyramidalization angle of carbon C(1) or C(5) in the cyclopentadienyl moiety, which is connected to the bis-pyrazolyl fragment. Indeed, when the ligand coordinates to the metal, it bends more in the case of titanium than it does with lithium, as indicated in Table 3, and at the same time the C(1) or C(5) atom acquires a non-negligible degree of pyramidalization. Such a deformation in the ligand structure is not very energetically demanding, as shown in Table 3. Note that a bond critical point (bcp) in the charge density¹⁶ was characterized between C(1) or C(5) and the two metal centers Li and Ti. Furthermore, although the bond distance is longer for titanium, the bond is stronger since the value of the charge density at the bcp is higher (0.039 e·au⁻³ for Ti, 0.019 e·au⁻³ for Li). A Mulliken population analysis showed a larger charge transfer from the ligand to the metal moiety in the titanium complex (see Table 3) in comparison to

Table 3. Deformation Energy of the Scorpionate Ligand, Energy Decomposition Analysis Terms ($\Delta E_{\text{int}} = \Delta E_{\text{elstat}} + \Delta E_{\text{Pauli}} + \Delta E_{\text{orb}}$, see ref 23), Charge Transferred to the Metallic Moiety (Δq), and Some Geometrical Parameters for Li(THF)⁺ and TiCl₃⁺ Model Complexes (values in kcal·mol⁻¹, electrons, and deg, respectively)

	Scorp-Li(THF)	Scorp-TiCl ₃
ligand deformation energy	+2.6	+7.0
Δ pyramidalization angle	6.5	8.5
Δ bending angle	4.4	7.
ΔE_{Pauli}	26.1	162.3
ΔE_{elstat}	-135.3	-229.8
ΔE_{orb}	-50.3	-200.3
ΔE_{int}	-159.5	-267.9
Δq	-0.29	-1.35

the lithium complex, probably a consequence of the different nature of the bonding. An energy decomposition analysis (EDA)²³ was performed and showed the different contributions to the bonding between the heteroscorpionate ligand and the metal moiety: ΔE_{elstat} and ΔE_{Pauli} account for the pure electrostatic interaction between the unperturbed electron densities of the isolated fragments and for the repulsion between electron pairs in the fragments, respectively; ΔE_{orb} is the energy associated with charge transfer and polarization of the fragments to reach the final situation in the molecule. It can be seen from the values in Table 3 that the Pauli repulsion is much larger between the titanium fragment and the ligand than in the case of lithium, as is the electrostatic interaction. Moreover, the sum of both terms (Pauli + elstat), which accounts for the total interaction between unperturbed fragments, is more favorable in the case of lithium (-109.2 kcal·mol⁻¹) than titanium (-67.5

(23) (a) Morokuma, K. *J. Chem. Phys.* **1971**, *55*, 1236–1238. (b) Ziegler, T.; Rauk, A. *Inorg. Chem.* **1979**, *18*, 1558–1565. (c) Ziegler, T.; Rauk, A. *Inorg. Chem.* **1979**, *18*, 1755–1759.

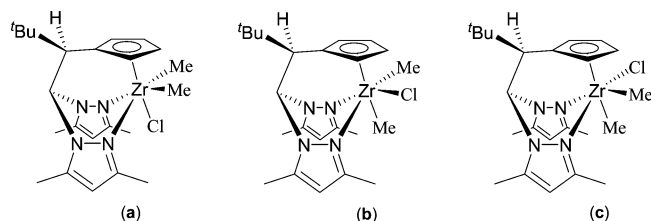


Figure 6. Proposed structures for the three possible diastereoisomers of complex **13**.

Table 4. Computed Relative Energies (in kcal·mol⁻¹) for the Isomers of Alkyl-Containing Ti, Zr, and Hf Compounds

		Ti		Zr		Hf	
a	b	a	b	a	b	a	b
		0.	+1.7	0.	+2.2	0.	+2.0
		0.	+5.0	0.	+1.6	+1.6	0.

kcal·mol⁻¹), and it is mainly dominated by electrostatic interactions. However, when the fragments are allowed to relax, the titanium moiety interacts more strongly with the ligand because, as mentioned above, the amount of charge transfer is larger. Titanium metal d orbitals mix efficiently with ligand electrons, while the lithium empty shell does not. Therefore, the titanium fragment interacts much more strongly with the ligand through donor–acceptor interactions, while the interaction between the ligand and lithium is mainly electrostatic and has negligible charge transfer.

Reactivity Studies. Alkyl derivatives of scorpionate-containing group 4 metal complexes are relatively rare,²⁴ although several examples of alkyl-containing half-sandwich group 4 metal complexes have been documented.² We proceeded to explore the synthesis of alkyl derivatives starting from one of the scorpionate/cyclopentadienyl group 4 metal complex described above. However, the alkylation of [ZrCl₃(bpztcP)] (**9**) with alkyl magnesium bromide reagents, such as MeMgBr or EtMgBr, in different molar ratios proved unsuccessful. Furthermore, treatment of **9** with 1 equiv of MeLi gave a complex mixture of products that could not be separated, but when this reaction was carried out in a 1:2 or 1:3 molar ratio, the dialkyl and the trialkyl complexes [ZrClMe₂(bpztcP)] (**13**) and [ZrMe₃(bpztcP)] (**14**), respectively, were isolated as white solids in low yields (25% and 30%, respectively) (see Scheme 7).

The ¹H and ¹³C{¹H} NMR spectra of the dialkyl complex **13** show two resonances for each of the H⁴, Me³, and Me⁵ pyrazole groups, indicating that in this case the two pyrazole rings are not equivalent and that in solution only one of the three possible diastereoisomers is present (see Figure 6). The response in the ¹H NOESY-1D experiment from the cyclopentadienyl protons on irradiating each of the alkyl groups suggests that this is the isomer in which the alkyl ligands are simultaneously in *cis* and *trans* positions to the nitrogen atoms of the pyrazole rings (**a** in Figure 6). Indeed, the relative stabilities of isomers **a** and **b** for the dialkyl derivatives (see Table 4) fully confirm the assignment of the NMR data. For the derivatives of the three metals, the chloride ligand sits *trans* to the cyclopentadienyl ring in the most stable isomer. Furthermore,

for the monoalkyl zirconium derivative, the difference in stability for the *cis* and *trans* isomers with regard to the cyclopentadienyl ligand is low. Since the difference in stability is maximized in the case of titanium, the calculations predict that in this instance the isolation of one single isomer would be expected. Although for the Zr and Hf derivatives the difference in energy between the two isomers is small, the relative stability is reversed for Hf.

The ¹H and ¹³C{¹H} NMR spectra of the trialkyl complex **14** also contain two resonances for each of the H⁴, Me³, and Me⁵ pyrazole groups. These results are consistent with an octahedral structural disposition with a κ²-NNη⁵-Cp scorpionate coordination with three methyl ligands occupying the other three coordination positions (see Scheme 7). Further experiments are in progress aimed at preparing new types of alkyl(aryl)-containing complexes and studying their reactivity toward unsaturated molecules such as isocyanides or Lewis acids.

Conclusions

The preparation of lithium derivatives of novel scorpionate/cyclopentadienyl ligands is described and involves an easy one-pot synthetic procedure based on the reaction of bis(3,5-dimethylpyrazol-1-yl)methane with BuⁿLi and fulvenes. However, the selection of appropriate substituents in the fulvene carbon atom is critical to enable the stabilization of the resulting lithium compounds. The potential utility of these ligands as valuable scaffolds in organometallic/coordination chemistry has been verified through the preparation of new group 4 metal complexes in which the ligands behave as tridentate systems with a κ²-N,N-η⁵-Cp coordination mode. In addition, the structures of both lithium and group 4 metal compounds were established on the basis of full geometry optimizations at a DFT level, and it was found that they agree very well with those determined by X-ray crystal structure studies. Furthermore, energy decomposition analysis (EDA) was carried out in order to evaluate the different contributions to the bonding between the ligand and the lithium and titanium moiety in these compounds. The results indicate that the titanium fragment interacts much more strongly through donor–acceptor interactions, while the interaction of the lithium fragment is mainly electrostatic in nature. We also explored the reactivity of one scorpionate/cyclopentadienyl zirconium complex, and new alkyl complexes were prepared. DFT-based calculations reproduced the molecular structures of these new compounds, and they supported the assignment of the isomers present in solution on the basis of their NMR data. Work is currently under way to increase the scope of this field.

Experimental Section

All reactions were performed using standard Schlenk-tube techniques under an atmosphere of dry nitrogen. Solvents were distilled from appropriate drying agents and degassed before use. Microanalyses were carried out with a Perkin-Elmer 2400 CHN analyzer. Mass spectra were recorded on a VG Autospec instrument using the FAB technique and nitrobenzyl alcohol as matrix. ¹H and ¹³C NMR spectra were recorded on a Varian Inova FT-500 spectrometer and referenced to the residual deuterated solvent. The NOESY-1D spectra were recorded with the following acquisition parameters: irradiation time 2 s and number of scans 256, using standard VARIANT-FT software. Two-dimensional NMR spectra were acquired using standard VARIANT-FT software and processed using an IPC-Sun computer.

The compounds TiCl₄(THF)₂, ZrCl₄, HfCl₄, 6,6-diphenylfulvene, and 6,6-dimethylfulvene were purchased from Aldrich. The compounds 6-*tert*-butylfulvene,¹² 6-phenylfulvene,¹² and bdmpzm [bd-

(24) (a) Milione, S.; Bertolasi, V.; Cuenca, T.; Grassi, A. *Organometallics* **2005**, *24*, 4915–4925. (b) Reger, R.; Tarquini, M. E.; Lebioda, L. *Organometallics* **1983**, *2*, 1763–1769. (c) Lee, H.; Jordan, R. F. *J. Am. Chem. Soc.* **2005**, *127*, 9384–9385. (d) Ipaktschi, J.; Sulzbach, W. J. *Organomet. Chem.* **1992**, *426*, 59–70.

mpzm = bis(3,5-dimethylpyrazol-1-yl)methane]¹¹ were prepared as reported previously.

Synthesis of [Li(bpzcp)(THF)] (1). In a 250 cm³ Schlenk tube, bdmpzm (1.00 g, 4.89 mmol) was dissolved in dry THF (70 cm³) and cooled to -70 °C. A 1.6 M solution of BuⁿLi (3.06 cm³, 4.89 mmol) in hexane was added, and the suspension was stirred for 1 h. The reaction mixture was warmed to 0 °C, and the resulting yellow suspension was treated with 6,6-diphenylfulvene (0.75 g, 4.89 mmol), after which the solution was stirred for 10 min. The solvent was removed to give a volume of 10 cm³, and on addition of hexane (70 cm³) a white solid was obtained. This solid was crystallized from a mixture of THF/hexane. Yield: 86%. Anal. Calcd for C₃₃H₃₇LiN₄O: C, 77.32; H, 7.27; N, 10.93. Found: C, 77.43; H, 7.28; N, 10.55. ¹H NMR (CD₃CN, 297 K): δ 7.20 (s, 1 H, CH), 5.77 (s, 2 H, H⁴), 2.02 (s, 6 H, Me³), 2.05 (s, 6 H, Me⁵), 7.43–7.09 (m, 10 H, Ph), 5.68 (m, 2 H, H²_{Cp}), 5.20 (m, 2 H, H³_{Cp}), 3.66 (m, 4 H, THF), 1.86 (m, 4 H, THF). ¹³C{¹H} NMR (CD₃CN, 297 K): δ 73.6 (CH), 147.6, 141.1 (C³ or ⁵), 106.2 (C⁴), 11.6 (Me³), 13.6 (Me⁵), 149.9, 131.0, 128.0, 126.4 (Ph), 63.1 (C^a), 113.7 (C¹_{Cp}), 101.9 (C²_{Cp}), 113.8 (C³_{Cp}), 68.2, 26.2 (THF). ⁷Li NMR (CD₃CN, 297 K): δ 1.21 (s). MS (*m/z* assignment, % intensity): 440 [Li-(bpzcp)], 100.

Synthesis of [Li(bpztcp)(THF)] (2). The synthetic procedure was the same as for complex **1**, using bdmpzm (1.00 g, 4.89 mmol), a 1.6 M solution of BuⁿLi (3.06 cm³, 4.89 mmol), and 6-*tert*-butylfulvene (0.66 g, 4.89 mmol), to give **2** as an orange solid. Yield: 90%. Anal. Calcd for C₂₅H₃₇LiN₄O: C, 72.11; H, 8.89; N, 13.46. Found: C, 72.24; H, 8.91; N, 13.25. ¹H NMR (CD₃CN, 297 K): δ 6.66 (s, 1 H, CH), 5.85 (s, 1 H, H⁴), 5.84 (s, 1 H, H⁴), 2.15 (s, 3 H, Me³), 2.07 (s, 3 H, Me⁵), 2.44 (s, 6 H, Me^{5,5'}), 2.95 (s, 1H, CH^a), 1.05 [s, 9 H, C(CH₃)₃], 4.95 (m, 1 H, H²_{Cp}), 5.50 (m, 1 H, H³_{Cp}), 5.70 (m, 1 H, H⁴_{Cp}), 5.58 (m, 1 H, H⁵_{Cp}), 3.68 (m, 4 H, THF), 1.84 (m, 4 H, THF). ¹³C{¹H} NMR (CD₃CN, 297 K): δ 66.8 (CH), 147.2, 147.1, 140.3, 138.2 (C^{3,3'} or ^{5,5'}), 106.0 (C⁴), 105.6 (C⁴), 13.3 (Me³), 13.2 (Me⁵), 12.0, 11.2 (Me^{5,5'}), 60.6 (C^a), 35.4 [C(CH₃)₃], 29.6 [C(CH₃)₃], 107.5 (C¹_{Cp}), 112.5 (C²_{Cp}), 107.1 (C³_{Cp}), 104.0 (C⁴_{Cp}), 100.9 (C⁵_{Cp}), 68.2, 26.1 (THF). ⁷Li NMR (CD₃CN, 297 K): δ 1.35 (s). MS (*m/z* assignment, % intensity): 416 [Li-(bpztcp)(THF)], 100.

Synthesis of a Mixture of Isomers 3a and 3b (bpzcpH). The synthetic procedure was the same as for complex **1**, using bdmpzm (1.00 g, 4.89 mmol), a 1.6 M solution of BuⁿLi (3.06 cm³, 4.89 mmol), and 6-phenylfulvene (0.75 g, 4.89 mmol), to give **3** as a white solid. Yield: 81%. Anal. Calcd for C₂₃H₂₆N₄: C, 77.06; H, 7.31; N, 15.63. Found: C, 77.11; H, 7.45; N, 15.25. ¹H NMR (CD₃-CN, 297 K): δ 6.73 (d, *J*_{HH} = 8.8 Hz, 1 H, CH), 6.70 (d, *J*_{HH} = 8.8 Hz, 1 H, CH), 5.75 (s, 1 H, H⁴), 5.73 (s, 1 H, H⁴), 5.52 (s, 2 H, H⁴), 2.41 (s, 3 H, Me³), 2.40 (s, 3 H, Me³), 2.19 (s, 3 H, Me³), 2.18 (s, 3 H, Me³), 2.11 (s, 3 H, Me⁵), 2.10 (s, 3 H, Me⁵), 2.04 (s, 3 H, Me⁵), 2.03 (s, 3 H, Me⁵), 5.73 (s, 1H, CH^a), 5.54 (s, 1H, CH^a), 7.33–7.15 (m, 10 H, Ph), 6.40–6.00 (m, 6 H, CH-Cp), 2.82 (br s, 2 H, CH₂-Cp), 2.75 (br s, 2 H, CH₂-Cp). ¹³C{¹H} NMR (CD₃CN, 297 K): δ 73.7, 73.5 (CH), 148.9, 148.7, 147.9, 146.4, 141.2, 140.9, 140.5, 140.2 (C³ or ⁵), 107.0, 106.9, 106.2 (C⁴), 13.6, 13.5, 13.4, (Me³), 11.7, 11.3 (Me⁵), 128.7–127.0 (Ph), 50.5, 50.1 (C^a), 128.9, 127.6 (C-Cp), 134.6, 134.3, 127.8, 127.6 (CH-Cp), 43.6, 42.1 (CH₂-Cp).

Synthesis of [Li(isoprⁿcp)]·bdmpzm·THF (4). The synthetic procedure was the same as for complex **1**, using bdmpzm (1.00 g, 4.89 mmol), a 1.6 M solution of BuⁿLi (3.06 cm³, 4.89 mmol), and 6,6-dimethylfulvene (0.52 g, 4.89 mmol), to give **4** as a white solid. Yield: 87%. Anal. Calcd for C₂₃H₃₃LiN₄O: C, 71.11; H, 8.56; N, 14.42. Found: C, 71.43; H, 8.74; N, 14.19. ¹H NMR (CD₃-CN, 297 K): δ 5.96 (s, 2 H, CH₂), 5.87 (s, 2 H, H⁴), 2.13 (s, 6 H, Me³), 2.43 (s, 6 H, Me⁵), 2.01 (s, 3H, MeC=), 4.81, 4.31 (two singlets, 1H, 1H, =CH₂), 5.76 (m, 2 H, H_{Cp}), 5.51 (m, 2 H, H_{Cp}), 3.68 (m, 4 H, THF), 1.84 (m, 4 H, THF). ¹³C{¹H} NMR (CD₃CN,

297 K): δ 58.4 (CH₂), 149.4, 140.8 (C³ or ⁵), 106.1 (C⁴), 12.8 (Me³), 10.4 (Me⁵), 21.2 (MeC=), 85.7 (MeC=), 98.5 (=CH₂), 121.6, 102.5, 104.8 (C_{Cp}), 68.5, 26.1 (THF).

Synthesis of [TiCl₃(bpzcp)] (5). To a cooled (-70 °C) THF (50 cm³) solution of TiCl₄(THF)₂ (0.50 g, 1.49 mmol) was added an equimolar quantity of [Li(bpzcp)(THF)] (**1**) (0.76 g, 1.49 mmol). The solution was stirred for 12 h at low temperature. The solvent was removed under vacuum and the solid extracted with CH₂Cl₂. A red solid was obtained after removal of the solvents. Yield: 90%. Anal. Calcd for C₂₉H₂₉Cl₃N₄Ti: C, 59.26; H, 4.97; N, 9.53. Found: C, 59.57; H, 5.08; N, 9.35. ¹H NMR (CDCl₃, 293 K): δ 6.99 (s, 1 H, CH), 6.01 (s, 2 H, H⁴), 2.19 (s, 6 H, Me³), 2.43 (s, 6 H, Me⁵), 7.35–7.25 (m, 10 H, Ph), 6.99 (m, 2 H, H^{2,5}_{Cp}), 6.08 (m, 2 H, H^{3,4}_{Cp}). ¹³C{¹H} NMR (CDCl₃): δ 72.8 (CH), 146.8, 129.2 (C³ or ⁵), 106.3 (C⁴), 15.8 (Me³), 11.0 (Me⁵), 149.9–113.1 (Ph), 68.8 (C^a), 111.3 (C¹_{Cp}), 122.0 (C^{2,5}_{Cp}), 113.8 (C^{3,4}_{Cp}). MS [FAB (*m/z* assignment, % intensity)]: 551 [M - Cl].

Synthesis of [ZrCl₃(bpzcp)] (6). The synthetic procedure was the same as for complex **5**, using ZrCl₄ (0.50 g, 2.14 mmol) and [Li(bpzcp)(THF)] (**1**) (1.09 g, 2.14 mmol), to give **6** as a red solid. Yield: 93%. Anal. Calcd for C₂₉H₂₉Cl₃N₄Zr: C, 55.14; H, 4.52; N, 8.87. Found: C, 55.26; H, 4.66; N, 8.95. ¹H NMR (CDCl₃, 293 K): δ 7.18 (s, 1 H, CH), 6.01 (s, 2 H, H⁴), 2.16 (s, 6 H, Me³), 2.68 (s, 6 H, Me⁵), 7.27–6.88 (m, 10 H, Ph), 7.26 (m, 2 H, H^{2,5}_{Cp}), 5.97 (m, 2 H, H^{3,4}_{Cp}). ¹³C{¹H} NMR (CDCl₃): δ 72.9 (CH), 143.9, 142.9 (C³ or ⁵), 110.5 (C⁴), 17.8 (Me³), 12.4 (Me⁵), 156.9–128.8 (Ph), 58.6 (C^a), 122.9 (C¹_{Cp}), 118.7 (C^{2,5}_{Cp}), 126.2 (C^{3,4}_{Cp}). MS [FAB (*m/z* assignment, % intensity)]: 595 [M - Cl].

Synthesis of [HfCl₃(bpzcp)] (7). The synthetic procedure was the same as for complex **5**, using HfCl₄ (0.50 g, 1.56 mmol) and [Li(bpzcp)(THF)] (**1**) (0.80 g, 1.56 mmol), to give **7** as a red solid. Yield: 90%. Anal. Calcd for C₂₉H₂₉Cl₃HfN₄: C, 48.48; H, 4.07; N, 7.80. Found: C, 48.58; H, 4.23; N, 7.75. ¹H NMR (CDCl₃, 293 K): δ 6.23 (s, 1 H, CH), 6.01 (s, 2 H, H⁴), 2.18 (s, 6 H, Me³), 2.59 (s, 6 H, Me⁵), 7.35–7.24 (m, 10 H, Ph), 6.90 (m, 2 H, H^{2,5}_{Cp}), 5.80 (m, 2 H, H^{3,4}_{Cp}). ¹³C{¹H} NMR (CDCl₃): δ 73.1 (CH), 145.8, 129.9 (C³ or ⁵), 106.4 (C⁴), 13.8 (Me³), 11.2 (Me⁵), 130.9–112.9 (Ph), 68.9 (C^a), 112.3 (C¹_{Cp}), 123.9 (C^{2,5}_{Cp}), 121.2 (C^{3,4}_{Cp}). MS [FAB (*m/z* assignment, % intensity)]: 682 [M - Cl].

Synthesis of [TiCl₃(bpztcp)] (8). The synthetic procedure was the same as for complex **5**, using TiCl₄(THF)₂ (0.50 g, 1.49 mmol) and [Li(bpztcp)(THF)] (**2**) (0.62 g, 1.49 mmol), to give **8** as an orange solid. Yield: 95%. Anal. Calcd for C₂₁H₂₉Cl₃N₄Ti: C, 51.30; H, 5.94; N, 11.39. Found: C, 51.65; H, 6.02; N, 11.11. ¹H NMR (CDCl₃, 293 K): δ 6.63 (s, 1 H, CH), 5.77 (s, 1 H, H⁴), 5.48 (s, 1 H, H⁴), 2.21 (s, 3 H, Me³), 2.08 (s, 3 H, Me³), 2.47 (s, 3 H, Me⁵), 2.31 (s, 3 H, Me⁵), 2.76 (s, 1H, CH^a), 0.80 [s, 9 H, C(CH₃)₃], 6.39 (m, 1 H, H⁵_{Cp}), 6.28 (m, 1 H, H²_{Cp}), 6.14 (m, 2 H, H^{3,4}_{Cp}). ¹³C{¹H} NMR (CDCl₃, 297 K): δ 72.1 (CH), 147.1, 145.8, 138.3, 138.2 (C^{3,3'} or ^{5,5'}), 106.9 (C⁴), 105.2 (C⁴), 13.9 (Me³), 13.6 (Me³), 12.1, 11.9 (Me^{5,5'}), 51.5 (C^a), 34.8 [C(CH₃)₃], 28.7 [C(CH₃)₃], 104.5 (C¹_{Cp}), 128.1 (C²_{Cp}), 125.5 (C⁵_{Cp}), 107.2, 105.1 (C^{3,4}_{Cp}). MS [FAB (*m/z* assignment, % intensity)]: 455 [M - Cl].

Synthesis of [ZrCl₃(bpztcp)] (9). The synthetic procedure was the same as for complex **5**, using ZrCl₄ (0.50 g, 2.14 mmol) and [Li(bpztcp)(THF)] (**2**) (0.89 g, 2.14 mmol), to give **9** as a pale orange solid. Yield: 85%. Anal. Calcd for C₂₁H₂₉Cl₃N₄Zr: C, 47.14; H, 5.46; N, 10.47. Found: C, 47.23; H, 5.61; N, 10.21. ¹H NMR (CDCl₃, 293 K): δ 6.76 (s, 1 H, CH), 6.07 (s, 1 H, H⁴), 5.98 (s, 1 H, H⁴), 2.65 (s, 3 H, Me³), 2.64 (s, 3 H, Me³), 2.59 (s, 3 H, Me⁵), 2.45 (s, 3 H, Me⁵), 2.83 (s, 1H, CH^a), 1.05 [s, 9 H, C(CH₃)₃], 7.32 (m, 1 H, H⁴_{Cp}), 7.06 (m, 1 H, H³_{Cp}), 5.90 (m, 1 H, H²_{Cp}), 5.85 (m, 1 H, H⁵_{Cp}). ¹³C{¹H} NMR (CDCl₃, 297 K): δ 65.5 (CH), 155.2, 154.9, 141.9, 138.9 (C^{3,3'} or ^{5,5'}), 110.3 (C⁴), 109.3 (C⁴), 17.4 (Me³), 17.2 (Me³), 12.7 (Me⁵), 11.8 (Me⁵), 55.7 (C^a), 34.8 [C(CH₃)₃], 28.3 [C(CH₃)₃], 119.2 (C¹_{Cp}), 130.7 (C⁴_{Cp}), 124.2

(C³_{Cp}), 118.5 (C²_{Cp}), 112.6 (C⁵_{Cp}). MS [FAB (*m/z* assignment, % intensity)]: 500 [M – Cl].

Synthesis of [HfCl₃(bpztcp)] (10). The synthetic procedure was the same as for complex **5**, using HfCl₄ (0.50 g, 1.56 mmol) and [Li(bpztcp)(THF)] (**2**) (0.65 g, 1.56 mmol), to give **10** as a pale orange solid. Yield: 90%. Anal. Calcd for C₂₁H₂₉Cl₃Hf N₄: C, 40.53; H, 4.70; N, 9.00. Found: C, 40.61; H, 4.87; N, 8.96. ¹H NMR (CDCl₃, 293 K): δ 6.67 (s, 1 H, CH), 6.01 (s, 1 H, H⁴), 5.92 (s, 1 H, H⁴), 2.64 (s, 3 H, Me³), 2.62 (s, 3 H, Me³), 2.50 (s, 3 H, Me⁵), 2.35 (s, 3 H, Me⁵), 2.72 (s, 1H, CH^a), 0.98 [s, 9 H, C(CH₃)₃], 7.11 (m, 1 H, H⁴_{Cp}), 6.86 (m, 1 H, H³_{Cp}), 5.67 (m, 1 H, H²_{Cp}), 5.62 (m, 1 H, H⁵_{Cp}). ¹³C{¹H} NMR (CDCl₃, 297 K): δ 66.0 (CH), 155.6, 155.4, 141.4, 138.3 (C^{3,3'} or ^{5,5'}), 110.6 (C⁴), 109.6 (C⁴), 17.8 (Me³), 17.6 (Me³), 12.7 (Me⁵), 11.7 (Me⁵), 55.8 (C^a), 34.9 [C(CH₃)₃], 28.3 [C(CH₃)₃], 115.8 (C¹_{Cp}), 129.0 (C⁴_{Cp}), 122.4 (C³_{Cp}), 116.3 (C²_{Cp}), 110.1 (C⁵_{Cp}). MS [FAB (*m/z* assignment, % intensity)]: 587 [M – Cl].

Synthesis of [ZrCl₃(bpzpcp)] (11). To a THF (50 cm³) solution of ZrCl₄ (0.50 g, 2.14 mmol) was added an equimolar quantity of the mixture of **3a** and **3b** (0.76 g, 2.14 mmol). The reaction mixture was heated under reflux and stirred for 12 h. The solvent was removed under vacuum, and the solid was washed with THF (20 cm³) and hexane (50 cm³) to yield **11** as a pale yellow solid. Yield: 75%. Anal. Calcd for C₂₃H₂₅Cl₃N₄Zr: C, 49.77; H, 4.54; N, 10.09. Found: C, 49.83; H, 4.68; N, 10.06. ¹H NMR (CDCl₃, 293 K): δ 6.49 (s, 1 H, CH), 6.09 (s, 1 H, H⁴), 6.06 (s, 1 H, H⁴), 2.78 (s, 3 H, Me³), 2.71 (s, 3 H, Me³), 2.51 (s, 3 H, Me⁵), 1.91 (s, 3 H, Me⁵), 4.62 (s, 1H, CH^a), 7.18–7.37 (m, 5 H, Ph), 7.36 (m, 1 H, H⁴_{Cp}), 6.92 (m, 1 H, H³_{Cp}), 6.08 (m, 1 H, H²_{Cp}), 5.89 (m, 1 H, H⁵_{Cp}). ¹³C{¹H} NMR (CDCl₃, 297 K): δ 69.5 (CH), 155.5, 154.9, 142.3, 136.8 (C^{3,3'} or ^{5,5'}), 109.8 (C⁴), 109.7 (C⁴), 17.3 (Me³), 17.1 (Me³), 12.0 (Me⁵), 11.4 (Me⁵), 50.8 (C^a), 130.1–127.5 (Ph), 119.0 (C¹_{Cp}), 129.6 (C⁴_{Cp}), 128.2 (C³_{Cp}), 116.3 (C⁵_{Cp}), 113.5 (C²_{Cp}). MS [FAB (*m/z* assignment, % intensity)]: 520 [M – Cl].

Synthesis of [HfCl₃(bpzpcp)] (12). The synthetic procedure was the same as for complex **11**, using HfCl₄ (0.50 g, 1.56 mmol) and the mixture of **3a** and **3b** (0.55 g, 1.56 mmol), to give **12** as an orange solid. Yield: 80%. Anal. Calcd for C₂₃H₂₅Cl₃HfN₄: C, 43.01; H, 3.92; N, 8.72. Found: C, 43.21; H, 3.98; N, 8.65. ¹H NMR (CDCl₃, 293 K): δ 6.35 (s, 1 H, CH), 6.10 (s, 1 H, H⁴), 6.08 (s, 1 H, H⁴), 2.81 (s, 3 H, Me³), 2.75 (s, 3 H, Me³), 2.47 (s, 3 H, Me⁵), 1.89 (s, 3 H, Me⁵), 4.58 (s, 1H, CH^a), 7.18–7.37 (m, 5 H, Ph), 7.37 (m, 1 H, H⁴_{Cp}), 6.98 (m, 1 H, H³_{Cp}), 5.98 (m, 1 H, H²_{Cp}), 5.78 (m, 1 H, H⁵_{Cp}). ¹³C{¹H} NMR (CDCl₃, 297 K): δ 68.2 (CH), 154.5, 152.6, 141.4, 135.8 (C^{3,3'} or ^{5,5'}), 107.8 (C⁴), 106.7 (C⁴), 15.3 (Me³), 14.9 (Me³), 12.8 (Me⁵), 11.9 (Me⁵), 58.3 (C^a), 130.1–127.5 (Ph), 115.8 (C¹_{Cp}), 132.6 (C⁴_{Cp}), 127.3 (C³_{Cp}), 113.2 (C⁵_{Cp}), 112.7 (C²_{Cp}). MS [FAB (*m/z* assignment, % intensity)]: 607 [M – Cl].

Synthesis of [ZrClMe₂(bpztcp)] (13). To a cooled (–20 °C) solution of [ZrCl₃(bpztcp)] (**9**) (0.50 g, 0.94 mmol) in dry THF (20 cm³) was added dropwise a 1.6 M solution of MeLi in diethyl ether (1.17 cm³, 1.88 mmol). The reaction mixture was stirred for 15 min at low temperature. The solvent was removed under vacuum, and the solid was extracted with toluene. The volatiles were removed under vacuum to give a pale orange solid, which was washed with hexane (2 × 10 cm³) to afford **23** as a pale yellow solid. Yield: 25%. Anal. Calcd for C₂₃H₃₅ClN₄Zr: C, 55.89; H, 7.14; N, 11.34. Found: C, 55.99; H, 7.40; N, 11.10. ¹H NMR (CDCl₃, 293 K): δ 6.55 (s, 1 H, CH), 5.93 (s, 1 H, H⁴), 5.86 (s, 1 H, H⁴), 2.49 (s, 3 H, Me³), 2.45 (s, 3 H, Me³), 2.48 (s, 3 H, Me³), 2.35 (s, 3 H, Me⁵), 2.80 (CH^a), 1.03 [s, 9 H, C(CH₃)₃], 6.90 (m, 1 H, H⁴_{Cp}), 6.58 (m, 1 H, H⁵_{Cp}), 5.77 (m, 1 H, H³_{Cp}), 5.74 (m, 1 H, H²_{Cp}), 0.50 (s, 3 H, Me), 0.45 (s, 3 H, Me). ¹³C{¹H} NMR (CDCl₃): δ 65.5 (CH), 154.4, 153.1, 140.6, 138.1 (C^{3,3'} or ^{5,5'}), 109.7 (C⁴), 108.8 (C⁴), 16.7, 16.5 (Me^{3,3'}), 12.7, (Me⁵), 11.8, (Me⁵),

56.8 (C^a), 35.2 [C(CH₃)₃], 28.7 [C(CH₃)₃], 116.7 (C¹_{Cp}), 129.3 (C³_{Cp}), 125.5 (C⁴_{Cp}), 116.8 (C²_{Cp}), 111.8 (C⁵_{Cp}), 28.4, 28.3 (Me', Me).

Synthesis of [ZrMe₃(bpztcp)] (14). The synthetic procedure was the same as for complex **23**, using [ZrCl₃(bpztcp)] (**9**) (0.50 g, 0.94 mmol) and MeLi (1.76 cm³, 2.82 mmol) to give **24** as a pale yellow solid. Yield: 29%. Anal. Calcd for C₂₄H₃₈N₄Zr: C, 60.84; H, 8.08; N, 11.82. Found: C, 60.91; H, 8.21; N, 11.58. ¹H NMR (CDCl₃, 293 K): δ 6.59 (s, 1 H, CH), 5.92 (s, 1 H, H⁴), 5.86 (s, 1 H, H⁴), 2.38 (s, 3 H, Me⁵), 2.35 (s, 3 H, Me⁵), 2.34 (s, 3 H, Me³), 2.29 (s, 3 H, Me³), 2.59 (CH^a), 0.98 [s, 9 H, C(CH₃)₃], 6.65 (m, 1 H, H⁴_{Cp}), 6.30 (m, 1 H, H⁵_{Cp}), 5.60 (m, 1 H, H³_{Cp}), 5.32 (m, 1 H, H²_{Cp}), 0.46, 0.20, 0.14 (s, 9 H, 3 Me–Zr). ¹³C{¹H} NMR (CDCl₃): δ 65.1 (CH), 153.1, 153.0, 140.5, 138.0 (C^{3,3'} or ^{5,5'}), 109.7 (C⁴), 108.5 (C⁴), 16.6, 16.4 (Me^{3,3'}), 15.7 (Me⁵), 14.3 (Me⁵), 56.8 (C^a), 35.3 [C(CH₃)₃], 25.8 [C(CH₃)₃], 114.9 (C¹_{Cp}), 121.7 (C³_{Cp}), 119.9 (C⁴_{Cp}), 115.7 (C²_{Cp}), 111.8 (C⁵_{Cp}), 46.9 (Me–Zr).

X-ray Crystallography. Suitable crystals of compounds **1**, **2**, **3b**, and **6** were mounted in glass capillaries and sealed under nitrogen. Crystallographic data are listed in Table 5. For **1** data were collected on a Nonius-Mach3 diffractometer using Mo K α radiation (graphite monochromator, $\lambda = 0.71073$ Å) with an $\omega/2\theta$ scan technique to a maximum value of 56°. The intensities were corrected in the usual fashion for Lorentz and polarization effects and empirical absorption correction was carried out on the basis of an azimuthal scan.²⁵

For **2**, **3b**, and **6**, data were collected on a Bruker SMART CCD-based diffractometer operating at 50 kV and 30 mA using 0.3° wide ω scans with a crystal-to-detector distance of 5.0 cm. The substantial redundancy in data allows empirical absorption corrections (SADABS²⁶) to be applied using multiple measurements of symmetry-equivalent reflections. The unit cell parameters were calculated and refined from the full data set. The raw intensity data frames were integrated with the SAINT²⁷ program, which also applied corrections for Lorentz and polarization effects.

For **1**, **2**, **3b**, and **6** the structures were solved by direct methods (SHELXS-97^{28a}), completed with difference Fourier syntheses, and refined with full-matrix least-squares using SHELXL-97^{28b} minimizing $w(F_o^2 - F_c^2)^2$. Weighted *R* factors (*R*_w) and all goodness of fit *S* are based on *F*²; conventional *R* factors (*R*) are based on *F*. All non-hydrogen atoms were refined with anisotropic displacement parameters. All scattering factors and anomalous dispersion factors are contained in the SHELXTL 6.10²⁹ program library. The hydrogen atom positions were calculated geometrically and were allowed to ride on their parent carbon atoms with fixed isotropic *U*.

Computational Details. All DFT calculations were carried out using the Amsterdam Density Functional (ADF2005.01) program developed by Baerends et al.³⁰ The numerical integration scheme

(25) North, A. C. T.; Phillips, D. C.; Mathews, F. S. *Acta Crystallogr. A* **1968**, 351–358.

(26) Sheldrick, G. M. *SADABS* version 2.03, a Program for Empirical Absorption Correction; Universität Göttingen, 1997–2001.

(27) *SAINTE+ NT* ver. 6.04, SAX Area-Detector Integration Program; Bruker AXS: Madison, WI, 1997–2001.

(28) (a) Sheldrick, G. M. *SHELXS-97*, Programs for Crystal Structure Analysis (Release 97-2); Institut für Anorganische Chemie der Universität: Göttingen, Germany, 1997. (b) Sheldrick, G. M. *SHELXL-97*, Programs for Crystal Structure Analysis (Release 97-2); Institut für Anorganische Chemie der Universität: Göttingen, Germany, 1997.

(29) Bruker AXS. *SHELXTL* version 6.10, Structure Determination Package; Bruker AXS: Madison, WI, 2000.

(30) (a) Baerends, E. J.; Ellis, D. E.; Ros, P. *Chem. Phys.* **1973**, 2, 41–51. (b) Baerends, E. J.; Ros, P. *Chem. Phys.* **1973**, 2, 52–59. (c) Baerends, E. J.; et al. *ADF2004.01*; SCM, Theoretical Chemistry, Vrije Universiteit: Amsterdam, The Netherlands, 2004; <http://www.scm.com>. (d) Guerra, C. F.; Snijders, J. G.; te Velde, G.; Baerends, E. J. *Theor. Chem. Acc.* **1998**, 99, 391–403.

Table 5. Crystal Data and Structure Refinement for **1**, **2**, **3b**, and **6**

	1	2	3b	6
empirical formula	C ₃₃ H ₃₇ LiN ₄ O	C ₂₅ H ₃₇ LiN ₄ O	C ₂₃ H ₂₆ N ₄	C ₂₉ H ₂₉ Cl ₃ N ₄ Zr·2THF
fw	512.61	416.53	358.48	775.34
temp (K)	250(2)	173(2)	100(2)	173(2)
wavelength (Å)	0.71073	0.71073	0.71073	0.71073
cryst syst, space group	monoclinic <i>P2(1)/a</i>	monoclinic <i>P2(1)/n</i>	triclinic <i>P</i>	monoclinic <i>P2(1)/n</i>
<i>a</i> (Å)	16.576(3)	8.980(1)	8.933(1)	12.222(1)
<i>b</i> (Å)	11.509(4)	15.405(2)	9.630(1)	23.628(2)
<i>c</i> (Å)	17.059(2)	17.817(3)	12.151(2)	12.889(1)
α (deg)			106.294(3)	
β (deg)	115.36(2)	98.094(3)	96.654(3)	100.935(2)
χ (deg)			94.664(3)	
volume (Å ³)	2941(12)	2440.1(6)	994.5(9)	3654.6(6)
Z, calcd density (g/cm ³)	4, 1.158	4, 1.134	2, 1.203	4, 1.409
absorp coeff (cm ⁻¹)	0.70	0.69	0.73	5.58
<i>F</i> (000)	1096	904	384	1608
cryst size (mm)	0.30 × 0.20 × 0.20	0.24 × 0.22 × 0.16	0.23 × 0.18 × 0.17	0.34 × 0.15 × 0.13
θ range for data collection	2.21 to 25.00	1.76 to 26.39	1.76 to 28.31	1.72 to 26.39
limiting indices	-19 ≤ <i>h</i> ≤ 17 0 ≤ <i>k</i> ≤ 13 0 ≤ <i>l</i> ≤ 20	-11 ≤ <i>h</i> ≤ 11 -19 ≤ <i>k</i> ≤ 19 -22 ≤ <i>l</i> ≤ 15	-11 ≤ <i>h</i> ≤ 11 -12 ≤ <i>k</i> ≤ 12 -16 ≤ <i>l</i> ≤ 16	-15 ≤ <i>h</i> ≤ 14 -21 ≤ <i>k</i> ≤ 29 -13 ≤ <i>l</i> ≤ 16
no. of reflns collected/unique	5290/5107 [<i>R</i> (int) = 0.0805]	10 415/4995 [<i>R</i> (int) = 0.0600]	13 538/4883 [<i>R</i> (int) = 0.0513]	20 933/7472 [<i>R</i> (int) = 0.0454]
no. of data/restraints/params	5107/0/352	4995/0/280	4883/0/248	7472/0/399
goodness-of-fit on <i>F</i> ²	0.902	1.025	1.058	1.038
final <i>R</i> indices [<i>I</i> > 2σ(<i>I</i>)]	<i>R</i> 1 = 0.0745 w <i>R</i> 2 = 0.1333	<i>R</i> 1 = 0.0647 w <i>R</i> 2 = 0.1574	<i>R</i> 1 = 0.0754 w <i>R</i> 2 = 0.1918	<i>R</i> 1 = 0.0538 w <i>R</i> 2 = 0.1530
<i>R</i> indices (all data)	<i>R</i> 1 = 0.3313 w <i>R</i> 2 = 0.1996	<i>R</i> 1 = 0.1421 w <i>R</i> 2 = 0.1894	<i>R</i> 1 = 0.1344 w <i>R</i> 2 = 0.2199	<i>R</i> 1 = 0.0837 w <i>R</i> 2 = 0.1716
largest diff peak and hole (e ⁻ Å ⁻³)	0.231 and -0.199	0.476 and -0.265	1.034 and -0.335	1.430 and -0.553

applied for the calculations was developed by te Velde et al.³¹ The geometry optimization procedure was based on the method reported by Versluis and Ziegler.³² The BP86 functional described as a combination between local VWN exchange–correlation potential with nonlocal Becke's exchange correction³³ and Perdew's correlation correction was used.³⁴ Relativistic corrections were introduced by scalar-relativistic zero-order regular approximation (ZO-RA).³⁵ A triple- ξ plus two polarization basis set was used for Ti, Zr, and Hf atoms and a plus one polarization function for the other atoms. For non-hydrogen and non-lithium atoms a relativistic frozen-core potential was used, including 2p for Ti, 3d for Zr, 4d for Hf, 2p for chlorine, and 1s for carbon and oxygen. A numerical integration parameter of 4.5 was employed in optimization and single-point calculations. Geometry convergence criteria were raised

1 order of magnitude to 10⁻³ hartree·Å⁻¹. Symmetry constraints were not used. The topological analysis of the electron density function was carried out using the Xaim program package.³⁶

Acknowledgment. We gratefully acknowledge financial support from the Ministerio de Educación y Ciencia (MEC), Spain (Grant Nos. CTQ2005-08123-CO2-01/BQU, BQU2002-04110-CO2-02, and CSD2006-0003) and the Junta de Comunidades de Castilla-La Mancha (Grant Nos. PAC-02-003, GC-02-010, and PAI-02-016). We are also indebted to the Generalitat de Catalunya (SGR01-00315) and to the ICIQ Foundation for financial support. M.U. thanks the Torres Quevedo program of the Ministerio de Educación y Ciencia, Spain.

Supporting Information Available: Details of data collection, refinement, atom coordinates, anisotropic displacement parameters, and bond lengths and angles for complexes **1**, **2**, **3b**, and **6**. This material is available free of charge via the Internet at <http://pubs.acs.org>.

OM7003942

(36) Ortiz Alba, J. C.; Bo, C. *Xaim-1.0*; Universitat Rovira I Virgili: Tarragona, Spain; <http://www.quimica.urv.es/XAIM>.

(31) (a) Boerrigter, P. M.; te Velde, G.; Baerends, E. J. *Int. J. Quantum Chem.* **1988**, *33*, 87–113. (b) te Velde, G.; Baerends, E. J. *J. Comput. Chem.* **1992**, *99*, 84–98.

(32) Versluis, L.; Ziegler, T. *J. Chem. Phys.* **1988**, *88*, 322–328.

(33) Becke, A. D. *Phys. Rev. A* **1988**, *38*, 3098–3100.

(34) (a) Perdew, J. P. *Phys. Rev. B* **1986**, *34*, 7406–7406. (b) Perdew, J. P. *Phys. Rev. B* **1986**, *33*, 8822–8824.

(35) (a) van Lenthe, E.; Baerends, E. J.; Snijders, J. G. *J. Chem. Phys.* **1993**, *99*, 4597–4610. (b) van Lenthe, E.; Baerends, E. J.; Snijders, J. G. *J. Chem. Phys.* **1994**, *101*, 9783–9792. (c) van Lenthe E.; Ehlers, A.; Baerends, E. J. *J. Chem. Phys.* **1999**, *110*, 8943–8953.